Chapter 2
Thermal Processes

Hua Shao, Tianyuan Zheng, Philipp Hein, Son Nguyen, Benoit Garitte, Thomas Nagel and Haibing Shao

2.1 Transient Heat Conduction in a Transversal Isotropic Porous Medium

Son Nguyen, Hua Shao, Benoit Garitte

The thermal field in the heating experiment in a bedded clay rock is the key driver for the hydraulic and mechanical response. It is therefore important to verify that the codes being used, COMSOL multiphysics and OGS can correctly calculate the temperature field. Due to low permeability of the clay rock, thermal conduction is the dominant process for the heat transfer. An analytical solution for a constant point heat source in an infinite transversely isotropic medium is used as a benchmark (Garitte et al. 2012).

H. Shao (✉)
BGR, Federal Institute for Geosciences and Natural Resources, Hannover, Germany
e-mail: hua.shao@bgr.de

T. Zheng (✉) · T. Nagel · H. Shao
UFZ, Helmholtz Centre for Environmental Research, Leipzig, Germany
e-mail: tianyuan.zheng@ufz.de

P. Hein (✉)
HTWK, Leipzig University of Applied Sciences, Leipzig, Germany
e-mail: philipp.hein@ufz.de

S. Nguyen
CNSC, Canadian Nuclear Safety Commission, Ottawa, Canada

B. Garitte
NAGRA, National Cooperative for the Disposal of Radioactive Waste, Wettingen, Switzerland

T. Nagel
Trinity College Dublin, Dublin, Ireland

H.B. Shao
Technische Universität Bergakademie Freiberg, Freiberg, Germany

O. Kolditz et al. (eds.), *Thermo-Hydro-Mechanical-Chemical Processes in Fractured Porous Media: Modelling and Benchmarking*, Terrestrial Environmental Sciences, DOI 10.1007/978-3-319-29224-3_2

2.1.1 Theory

Heat transfer including conduction, convection and radiation is the passage of thermal energy from a hot to a cold body. Transfer of thermal energy occurs, when a body and its surroundings have not yet reached thermal equilibrium yet. Conduction takes place when there is a temperature gradient in a solid. Consider a boundary value problem for heat conduction in a continuously non-homogeneous anisotropic medium, which is governed by the following equation:

$$\rho c_p \frac{\partial T}{\partial t} + \mathrm{div}(\boldsymbol{\lambda} \mathrm{grad} T) = q \tag{2.1.1}$$

where $T(x_i, t)$ is the temperature field, $q(x_i, t)$ is the heat sources. $\boldsymbol{\lambda}(x_i, t)$ is the thermal conductivity tensor and is defined to quantify the ease with which a particular medium conducts, $\rho(x_i)$ is the mass density and $c_p(x_i)$ the specific heat. The index i (=1, 2, and 3) instead of Cartesian coordinate system (x, y, z). The global boundary Γ consists of two parts $\Gamma = \Gamma_T + \Gamma_q$ (Γ_T Dirichlet and Γ_q Cauchy conditions).

2.1.2 Problem Definition

A cubic geometry with an edge length of 20 m × 20 m × 20 m is selected to present an infinite transversely isotropic medium. A constant heat source is applied in the middle of the cube. Due to the symmetrical geometry, only 1/8 of the cube is used for the simulation. The finite element model for this problem is shown in Fig. 2.1. The source is located at point (0, 0, 0). The initial temperature in the medium is 21.5 °C.

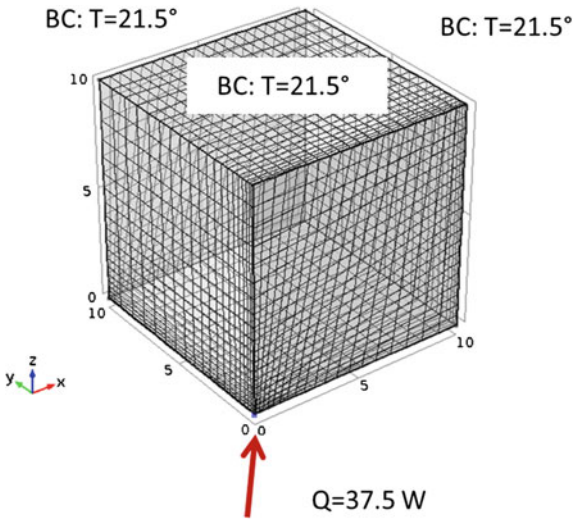

Fig. 2.1 Finite element mesh for the COMSOL-simulation

Table 2.1 Used parameters

	Quantity	Value/unit
ρ	Density of the solid	2.45 t m^3
c_p	Heat capacity	1000 J kg^{-1} K^{-1}
$\lambda\|\|$	Thermal conductivity in horizontal direction ($r = x, y$)	2.1 W m^{-1} K^{-1}
$\lambda\perp$	Thermal conductivity in vertical direction (z)	1 W m^{-1} K^{-1}

The outer boundaries are set at a distance of 10 m from the source where T is fixed at 21.5 °C. The finite element results are compared to the analytical solution at four points: two at horizontal distances of 0.5 and 2 m from the source, and two at vertical distances of 0.5 and 2 m. In this verification problem, the following parameters are considered (Table 2.1). The total simulation time is 10,000 days with variable time steps.

2.1.3 Analytical Solution

In case of constant parameters (Table 2.1), and taking into account of transversal isotropic medium, the thermal conductivity tensor $\boldsymbol{\lambda}(x_i)$ may follow:

$$\begin{aligned} \kappa_{xy} = \kappa_{xz} = \kappa_{yz} = \kappa_{zx} = \kappa_{zy} = \kappa_{yx} = 0 \\ \kappa_{xx} = \kappa_{yy} = \kappa_{\perp} \\ \kappa_{zz} = \kappa_{||} \end{aligned} \tag{2.1.2}$$

The analytical solution proposed by Booker and Savvidou (1985b) for a point heat source in an infinite isotropic medium of the heat conduction equation in the porous medium (Carslaw and Jaeger 1959) can be transformed to take anisotropy into account (Garitte et al. 2012):

$$\Delta T = \frac{q}{4\pi\lambda_0 R_0} \operatorname{erfc} \frac{R_0}{s\sqrt{\lambda_0 t/\rho c_p}} \tag{2.1.3}$$

where ΔT is the temperature increment induced by the applied power q (in W), λ_0 is the equivalent thermal conductivity (in W/m/K):

$$\lambda_0 = \sqrt[3]{\lambda_{||}\lambda_{||}\lambda_{\perp}} \tag{2.1.4}$$

and erfc() stands for the complementary error function. The solution is calculated in a Cartesian reference system where x- and y-axes are defined within the bedding plane and z perpendicular to the bedding. The transformed radius R_0 is a function of the isotropy-like distances ξ, η, ζ in x, y and z direction, respectively:

$$R_0 = \sqrt{\xi^2 + \eta^2 + \zeta^2} \tag{2.1.5}$$

where ξ, η, ζ are related to the real distances x, y and z through:

$$\begin{aligned} x &= \frac{\sqrt{\lambda_{||}}}{\sqrt{\lambda_0}}\xi \\ y &= \frac{\sqrt{\lambda_{||}}}{\sqrt{\lambda_0}}\eta \\ z &= \frac{\sqrt{\lambda_{\perp}}}{\sqrt{\lambda_0}}\zeta \end{aligned} \tag{2.1.6}$$

2.1.4 Results

The results of the analytical equation (2.1.3) for the temperature evolution at the selected points are compared to those of the numerical simulations by COMSOL and OGS (Fig. 2.2). The analytical solution is based on an infinite geometry assumption, therefore the boundary effects become more pronounced at later times in the

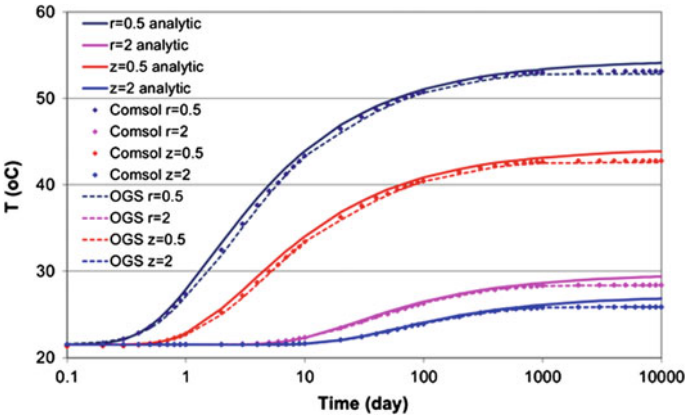

Fig. 2.2 Comparison of finite element and analytical results

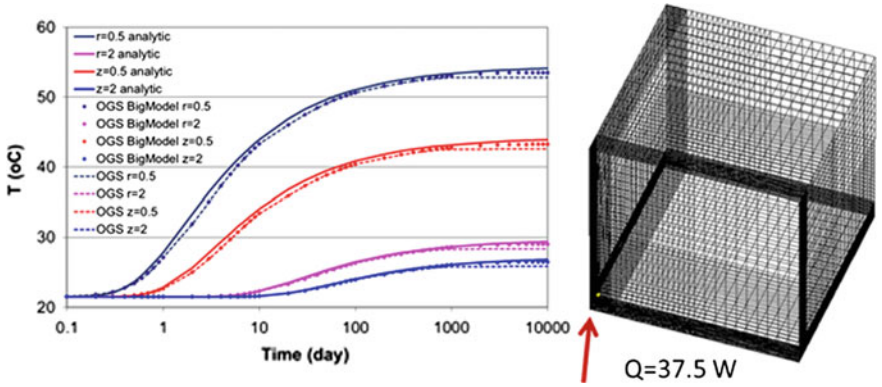

Fig. 2.3 OGS results from the big model

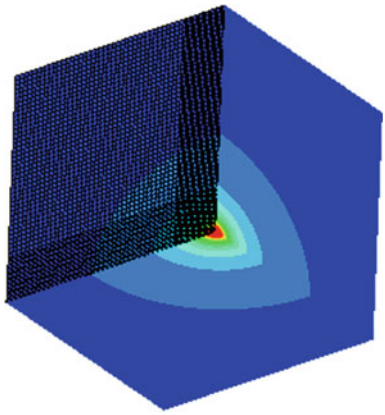

Fig. 2.4 Temperature distribution at 10,000 days calculated by code OGS

numerical simulations. The relative error between the modelled temperature and the result from analytical solution is about 4 %. A big model (40 m × 40 m × 40 m) with a relative coarse mesh improves the boundary effect (Fig. 2.3). Mesh effect plays also an important role. A much finer mesh for the OGS simulator seems to be needed in order to get comparable results.

Figure 2.4 shows the temperature distribution in domain at 10,000 days. Obviously, heat transfers much faster in the horizontal than in the vertical direction because of transversal isotropic thermal conductivity.

2.2 Freezing-Thawing

Tianyuan Zheng, Thomas Nagel and Haibing Shao

In this chapter, we are going to show how to simulate the heat transport process with freezing and thawing features. To handle such phase change behaviour, both kinetic and equilibrium approaches have been implemented into to the numerical model. The extended feature is verified by comparing the numerical results against analytical solutions.

2.2.1 Mathematical Model

Heat Conduction

Conventionally, when only considering heat conduction, the governing equation of the heat transport process reads,

$$\rho \frac{\partial h(T)}{\partial t} - \nabla \cdot (\boldsymbol{\lambda} \nabla T) = 0 \tag{2.2.1}$$

where $h(T)$ denotes the specific enthalpy [J/kg], ρ is the density [kg/m^3] of the porous media, T refers to the temperature [K], and $\boldsymbol{\lambda}$ is the thermal conductivity [W m^{-1} K^{-1}]. By applying the chain rule to the time derivative term, one gets

$$\rho \frac{\partial h}{\partial T} \frac{\partial T}{\partial t} - \nabla \cdot (\boldsymbol{\lambda} \nabla T) = 0 \tag{2.2.2}$$

The term $\frac{\partial h}{\partial T}$ represents the derivative of enthalpy with respect to temperature, which is equivalent to the specific heat capacity c_p [J kg^{-1} K^{-1}]. Equation (2.2.2) can be rewritten as

$$\rho c_{\mathrm{p}} \frac{\partial T}{\partial t} - \nabla \cdot (\boldsymbol{\lambda} \nabla T) = 0 \tag{2.2.3}$$

2.2.2 Freezing and Thawing Processes

Kinetic Approach

Based on the governing equation (2.2.3), thawing and freezing processes can be taken into account by quantifying the change of the apparent fluid density over time. When the temperature drops below the freezing point, part of the water in the pore space

is transformed into ice, leading to a drop in the apparent water density. In order to model this physical process, we first introduce the mass balance equation.

$$\dot{\rho}_\alpha + \nabla \cdot (\rho_\alpha \boldsymbol{v}_\alpha) = \hat{\rho}_\alpha \tag{2.2.4}$$

where $\dot{\rho}_\alpha$ represents the partial time derivative of the partial density of phase α, $\boldsymbol{v}_\alpha$ represents the velocity of phase α, and $\hat{\rho}_\alpha$ is the density production of phase α, which is caused by the phase change process. Since all phases are considered immobile in this model $\boldsymbol{v}_\alpha = 0$, thus for the ice phase Eq. (2.2.4) can be simplified as

$$\dot{\rho}_\mathrm{I} = \hat{\rho}_\mathrm{I} \tag{2.2.5}$$

For a simple freezing model, $\hat{\rho}_\mathrm{I}$ is assumed to be linearly dependent on the temperature difference from the freezing point temperature T_m to the current temperature T, with k referring to a non-negative rate coefficient [kg m^{-3} s^{-1} K^{-1}].

$$\hat{\rho}_\mathrm{I} = k(T_\mathrm{m} - T), \quad k \geq 0 \tag{2.2.6}$$

Here we define the ice volume fraction ϕ_I as the volume of ice over the total volume of REV, and it is constrained by the porosity ϕ, i.e. $\phi_\mathrm{I} \in [0, \phi]$. Equation (2.2.6) then becomes

$$\hat{\rho}_\mathrm{I} = k(T_\mathrm{m} - T) = \frac{\partial \phi_\mathrm{I} \rho_\mathrm{IR}}{\partial t} \tag{2.2.7}$$

where ρ_IR refers to the real density of ice. Then we can add the phase change term into Eq. (2.2.3).

$$\rho c_\mathrm{p} \frac{\partial T}{\partial t} - L_\mathrm{I} \hat{\rho}_\mathrm{I} - \nabla \cdot (\boldsymbol{\lambda} \nabla T) = 0, \tag{2.2.8}$$

where L_I denotes the latent heat [J kg^{-1}] and the term $L_\mathrm{I}\hat{\rho}_\mathrm{I}$ regulates the amount of energy released or absorbed through the phase change process. When freezing and thawing occur, $\boldsymbol{\lambda}$ and ρc_p are no longer constants, but rather functions of the ice volume fraction ϕ_I.

$$\boldsymbol{\lambda} = \boldsymbol{\lambda}_\mathrm{S}(1 - \phi) + \boldsymbol{\lambda}_\mathrm{I}(\phi_\mathrm{I}) + \boldsymbol{\lambda}_\mathrm{W}(\phi - \phi_\mathrm{I}) \tag{2.2.9}$$

$$\rho c_\mathrm{p} = \rho_\mathrm{SR} c_\mathrm{pS}(1 - \phi) + \rho_\mathrm{IR} c_\mathrm{pI}(\phi_\mathrm{I}) + \rho_\mathrm{WR} c_\mathrm{pW}(\phi - \phi_\mathrm{I}) \tag{2.2.10}$$

Equilibrium Approach

In the equilibrium approach, one follows the same governing equations as in the kinetic approach (Eqs. (2.2.1)–(2.2.8)). The difference lies in the calculation of the

ice phase density production $\hat{\rho}_{\mathrm{I}}$. Here, the phase change process is assumed to be very fast, and will reach equilibrium within a typical time step. Instead of calculating the phase production rate, the ice volume fraction is directly related to temperature, and is updated with a certain function before every time step. Assuming the partial density of ice is a function of temperature T, we have

$$\rho_{\mathrm{I}} = \rho_{\mathrm{eq}}(T) \tag{2.2.11}$$

$\rho_{\mathrm{eq}}(T)$ defines the relationship between partial density of ice and temperature, which can be regulated by either a sigmoid function

$$\rho_{\mathrm{I}} = \phi\rho_{\mathrm{IR}}\frac{1}{1+e^{-wt}} \tag{2.2.12}$$

or an exponential function which is also steadily differentiable (Fig. 2.5) (Mottaghy and Rath 2006).

$$\rho_{\mathrm{I}} = \begin{cases} \phi\rho_{\mathrm{I}} & \text{if} \quad T < T_{\mathrm{s}} \\ \phi\rho_{\mathrm{IR}}(1 - e^{-(\frac{T-T_{\mathrm{m}}}{w})^2}) & \text{if} \quad T < T_{\mathrm{m}} \\ 0 & \text{if} \quad T > T_{\mathrm{m}} \end{cases} \tag{2.2.13}$$

where T_{m} represents the melting temperature and T_{s} represents the temperature at which all water has frozen into ice. When freezing is taken into account, the specific enthalpy h is regarded as a function of T and ρ_{I}, one gets

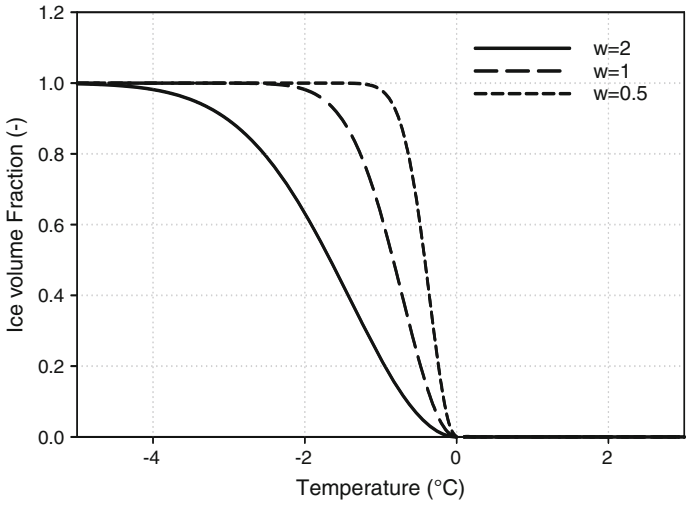

Fig. 2.5 Ice volume fraction versus temperature for exponential functions

$$\rho \frac{\partial h(T, \rho_\mathrm{I})}{\partial t} = \rho \left(\frac{\partial h}{\partial T}\bigg|_{\rho_\mathrm{I}} \frac{\partial T}{\partial t} + \frac{\partial h}{\partial \rho_\mathrm{I}}\bigg|_{T} \frac{\partial \rho_\mathrm{I}}{\partial t} \right). \tag{2.2.14}$$

By applying the chain rule on Eq. (2.2.14) and using Eq. (2.2.11), we get

$$\frac{\partial \rho_\mathrm{I}}{\partial t} = \frac{\partial \rho_\mathrm{eq}(T)}{\partial T} \frac{\partial T}{\partial t} \tag{2.2.15}$$

After integrating the above expressions into Eq. (2.2.8), we have

$$\left(\rho c_\mathrm{p} - \frac{\partial \rho_\mathrm{eq}}{\partial T} L_\mathrm{I} \right) \frac{\partial T}{\partial t} - \nabla \cdot (\boldsymbol{\lambda} \nabla T) = 0 \tag{2.2.16}$$

Equation (2.2.16) serves as the governing equation of the heat transport process with freezing and thawing features in the equilibrium approach.

2.2.3 *Benchmark Validation and Discussion*

Mottaghy and Rath (2006) proposed a benchmark case, with a 1 m long water column connected to a freezing wall. Over time, the water in the vicinity of the wall slowly freezes. The propogation of the freezing front is calculated by the Neumann analytical solution (Carslaw and Jaeger 1959) (see Appendix). In our numerical model, the Finite Difference Method was implemented for the time discretization. For the spatial discretization, we have adopted the Galerkin Finite Element Method, with 1000 line elements, each 1 cm long. Picard and Newton methods were introduced to resolve the nonlinearity. Since the analytical solution was developed for a pure phase change scenario, i.e. only water and ice, we set the porosity to be 1 in the numerical model. The initial temperature was given as 0 °C throughout the domain. For the boundary condition, the left hand side of the column x = 0 was constrained to a temperature value T = −3 °C throughout the simulation. All other parameters used in the model are listed in Table 2.2.

Figure 2.6 shows the evolution of temperature profile during the freezing process. The location of the phase change front $X(t)$ is compared with the analytical solution in Fig. 2.7. The red symbols are the numerical results and the blue line is the Neumann analytical solution (see Appendix for the details). Here, the exponential function was applied to calculate the partial density of ice in Eq. (2.2.13), with $\rho_\mathrm{IR} = 920\,\mathrm{kg\,m^{-3}}$, $w = 2$ and $T_\mathrm{s} = -4\,^\circ\mathrm{C}$. As shown in Fig. 2.7, the numerical results correspond well to the analytical solution.

Table 2.2 Parameters used in the benchmark case, following Mottaghy and Rath (2006)

Parameters	Values	Units
Grid size	0.001	m
Initial temperature	0	°C
Boundary temperature	−3	°C
Porosity	1	–
Water heat capacity	4179	J kg^{-1} K^{-1}
Water thermal conductivity	0.613	W m^{-1} K^{-1}
Water density	920	kg m^{-3}
Ice heat capacity	2052	J kg^{-1} K^{-1}
Ice thermal conductivity	2.14	W m^{-1} K^{-1}
Ice density	920	kg m^{-3}
Time step size	864	s
Total simulation time	100	day

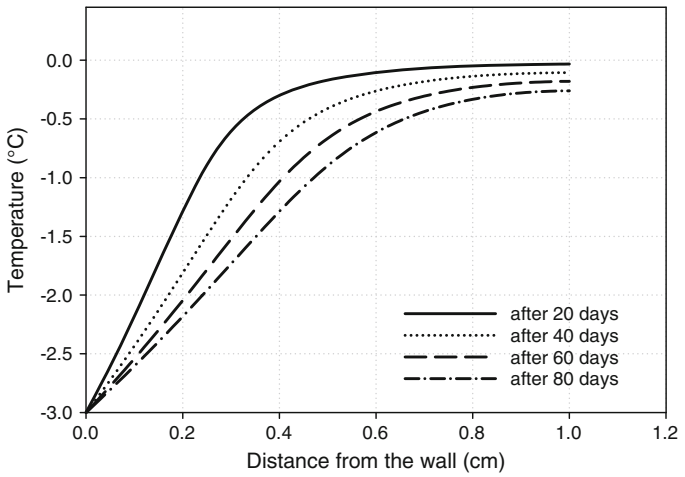

Fig. 2.6 The temperature field during the freezing process

Appendix

A classical solution for a semi-infinite medium with constant temperature to conductive heat transfer problems with solidification phase change was given by Neumann (1860) and has been expanded by Carslaw and Jaeger (1959). It is called the Neumann solution and specifies the location $X(t)$ of the phase front as a function of time.

$$X(t) = 2\gamma\sqrt{\alpha_1 t} \tag{2.2.17}$$

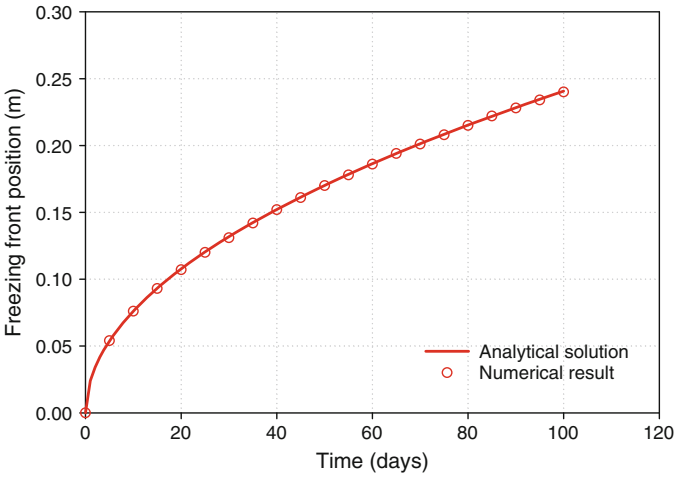

Fig. 2.7 Propagation of the freezing front X over time. The analytical solution by Neumann is depicted by the *red* line, and the numerical results are shown in *red* symbols

$\alpha_{\mathrm{I,W}}$ indicates the thermal diffusivity of ice and water respectively. The parameter γ must be determined from the following equation that related to the boundary condition of the associated differential equation (with the thermal conductivities $\lambda_{\mathrm{I,W}}$ of both materials)

$$\frac{\exp\left[\left(\alpha_{\mathrm{I}}-\alpha_{\mathrm{W}}\right)\gamma^2\right]\operatorname{erfc}\left(\gamma\sqrt{\alpha_{\mathrm{I}}/\alpha_{\mathrm{W}}}\right)}{\operatorname{erf}\left(\gamma\right)}-\frac{\left(T_{\mathrm{m}}-T_{\mathrm{s}}\right)\lambda_{\mathrm{W}}\sqrt{\alpha_{\mathrm{I}}}}{\left(T_{\mathrm{s}}-T_0\right)\lambda_{\mathrm{I}}\sqrt{\alpha_{\mathrm{W}}}}=0 \tag{2.2.18}$$

The latent heat for the phase change is considered by adding into the thermal diffusivity of the water.

$$\alpha_{\mathrm{W}}=\frac{\lambda w}{\rho_{\mathrm{W}}c_{\mathrm{W}}-\rho_{\mathrm{I}}L_{\mathrm{I}}\frac{\mathrm{d}\phi_{\mathrm{I}}}{\mathrm{d}T}} \tag{2.2.19}$$

In the numerical model we choose $w=2$ (Fig. 2.5) for the exponential function and the corresponding $\triangle T$ is 4 (see Table 2.3). Then $\gamma=0.039$ should be chosen for the analytical solution.

Table 2.3 The parameter γ for the different widths of freezing range (Mottaghy and Rath 2006)

γ	$\triangle T$ (°C)
0.039	4
0.041	3
0.043	2

2.3 Shallow Geothermal Systems—Borehole Heat Exchanger

Philipp Hein and Haibing Shao

To use the shallow geothermal resources, borehole heat exchangers are often coupled with heat pumps to provide heating or cooling in the buildings. The OpenGeoSys software has recently been extended to simulate the evolution of temperature profile within and around the BHEs. Here in this section, two benchmark cases are presented. One compares the simulated soil temperature curve to analytical line source models. The other one validates the numerical model against monitoring data from an in-door sandbox experiment.

2.3.1 Borehole Heat Exchangers—Comparison to Line Source Models

Model Setup

In this benchmark, the evolution of soil temperature was simulated by the numerical model OpenGeoSys. The results were compared against the analytical **infinite line source** (ILS) model (c.f. Stauffer et al. (2014)). As by the ILS model, the temperature difference to the undisturbed initial temperature T_0 at a radial distance r_b is given by

$$T - T_0 = \frac{q_b}{4\pi\lambda} E_1\left(\frac{r_b^2}{4\alpha t}\right) \tag{2.3.1}$$

with heat flow rate q_b per length of BHE, thermal diffusivity $\alpha = \frac{\lambda}{\rho c_p}$ and the exponential integral function E_1.

In the numerical model, the temperature evolution inside and around a BHE was simulated with a constant power $Q = q_b \cdot L_{BHE}$ imposed as a boundary condition. Both numerical and analytical models have been established with the same geometry, initial conditions, and material parameters etc. They are listed in Table 2.4. It is known that the analytical line source model will produce inaccurate results of soil temperature in the immediate vicinity of the BHE, still it should converge with the numerical model at a certain distance. The results are presented in the next section.

Results

Soil temperatures were observed at two locations, one at a distance of $r_1 = 6.0\,\text{m}$ and another at $r_2 = 1.6\,\text{m}$ (c.f. Fig. 2.8). Good agreement has been reached between

Table 2.4 Parameters used in the line source model comparison

Parameter	Value	Unit
q_b	-5.68	W m^{-1}
L_{BHE}	46	m
Q	-261.68	W
λ_{soil}	1.34	W m^{-1} K^{-1}
$(\rho c_p)_{soil}$	2×10^6	J m^{-3} K^{-1}
BHE Type	$1U$	
D_{BHE}	15	cm
d_{pipe}	3.98	cm
b_{pipe}	0.36	cm
w	6.3	cm
λ_{pipe}	0.39	W m^{-1} K^{-1}
λ_{grout}	0.73	W m^{-1} K^{-1}
$(\rho c_p)_{grout}$	3.8×10^6	J m^{-3} K^{-1}
$\lambda_{refrigerant}$	0.477	W m^{-1} K^{-1}
$(\rho c_p)_{refrigerant}$	3.838×10^6	J m^{-3} K^{-1}
$\mu_{refrigerant}$	3.04×10^{-3}	kg m^{-1} s^{-1}
$Q_{refrigerant}$	15.087	m^3 d^{-1}

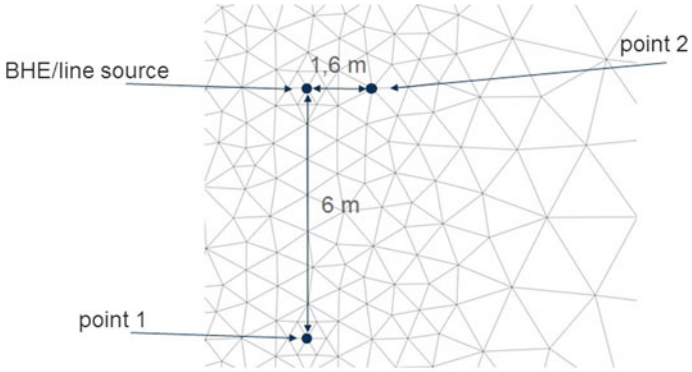

Fig. 2.8 Observation points in line source model

the analytical line source model solution and the numerical results. The comparison of temperature profiles can be found in Figs. 2.9 and 2.10.

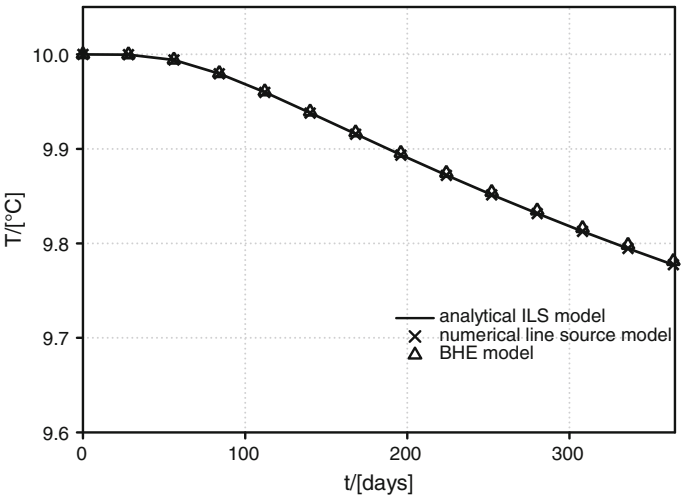

Fig. 2.9 Comparison of soil temperature profile at 6.0 m distance

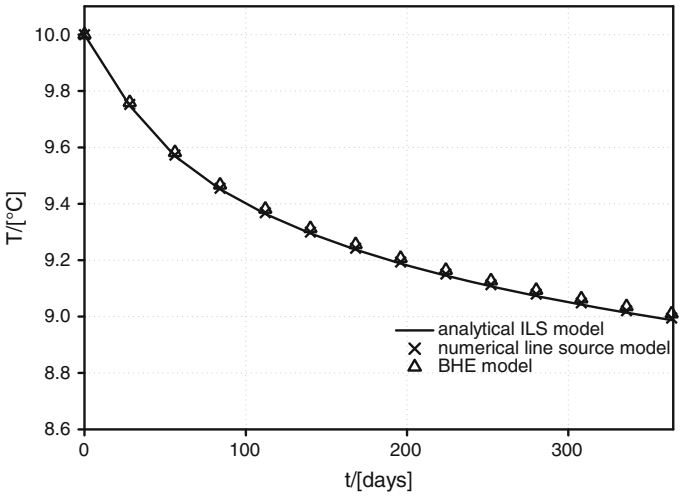

Fig. 2.10 Comparison of soil temperature profile at 1.6 m distance

2.3.2 Borehole Heat Exchangers—Sandbox Benchmark

In this benchmark, the Borehole Heat Exchanger (BHE) feature in the OpenGeoSys software is validated against experimental results obtained by Beier et al. (2011). In their experiment, a Thermal Response Test (TRT) was performed under controlled conditions on a single U-tube borehole heat exchanger placed inside a sand box.

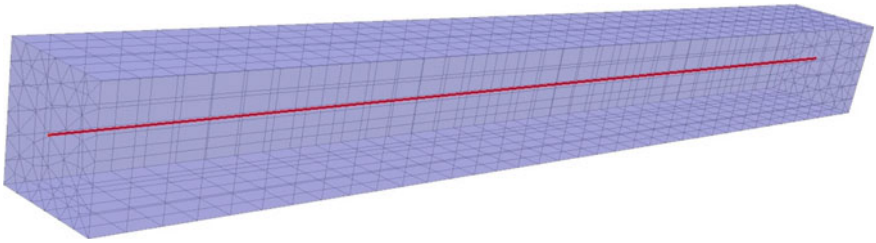

Fig. 2.11 Sandbox model

Inlet and outlet fluid temperatures were monitored together with temperatures at the borehole wall and at different locations in the sand box.

Model Setup

The model was built according to the experimental configurations. The BHE is represented by line elements which are embedded in a 3D prism mesh representing the sandbox (Fig. 2.11). The length of the box is 18 m with a square cross section of 1.8 m per side. Detailed parameters for the model configuration can be found in Table 2.5.

In Beier's experiment, there was an aluminium pipe acting as the borehole wall. It cannot be represented by the BHE model itself, therefore the borehole diameter was taken as the aluminium pipe's outer diameter of 0.13 m in the numerical model. The grout's thermal conductivity was increased from originally 0.73 to 0.806 W m^{-1} K^{-1}, in order to include the aluminium pipe's thermal conductivity and its geometry. The BHE is filled with water. Thermal properties and viscosity of water are taken at an average temperature of approx. 36 °C.

Table 2.5 Benchmark parameters according to the sandbox experiment of Beier et al. (2011)

Parameter	Value	Unit
λ_{soil}	2.78	W m^{-1} K^{-1}
$(\rho c_p)_{soil}$	3.2×10^6	J m^{-3} K^{-1}
D_{BHE}	13	cm
d_{pipe}	2.733	cm
b_{pipe}	0.3035	cm
w	5.3	cm
λ_{pipe}	0.39	W m^{-1} K^{-1}
λ_{grout}	0.806	W m^{-1} K^{-1}
$(\rho c_p)_{grout}$	3.8×10^6	J m^{-3} K^{-1}

Table 2.6 Initial conditions of sandbox model

Parameter	Value	Unit
T_{in}	22.21	ºC
T_{out}	21.98	ºC
T_{grout1}	22.08	ºC
T_{grout2}	21.97	ºC
T_{soil}	22.10	ºC
T_{wall}	21.95	ºC

Initial and Boundary Conditions

Initial conditions for fluid inlet/outlet temperatures and wall temperature were directly taken from the measurements at $t = 0$. For the initial soil temperature, the mean value of all sensors placed in the sand was taken. As initial grout temperatures, arithmetic mean between wall and fluid inlet/outlet temperature was taken. Detailed initial temperatures can be found in Table 2.6. For the boundary conditions, they are given on the BHE as time series of measured inlet fluid temperature and flow rate as demonstrated in Fig. 2.12.

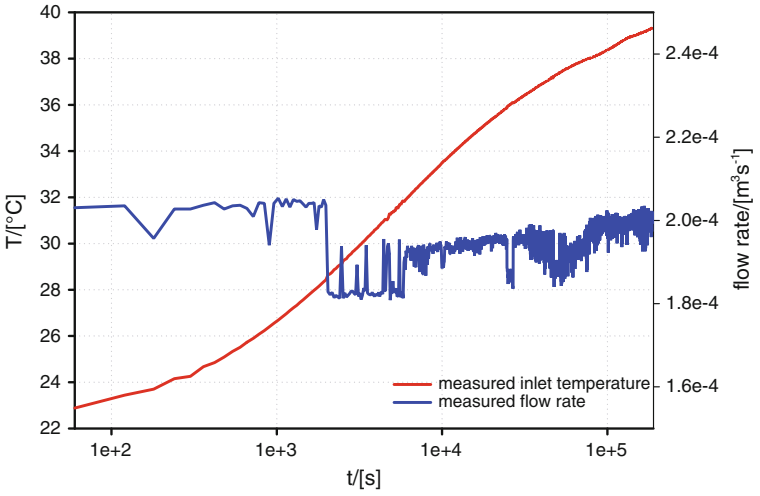

Fig. 2.12 Time series of inlet temperature and flow rate

Results

The outlet temperature (Fig. 2.13) as well as the borehole wall temperature and soil temperatures at 24 and 44 cm distance to the wall (Fig. 2.14) were compared to the experimental results. We can observe a good match between experimental and simulation results. The largest relative error is about 2.5 % on the wall temperature.

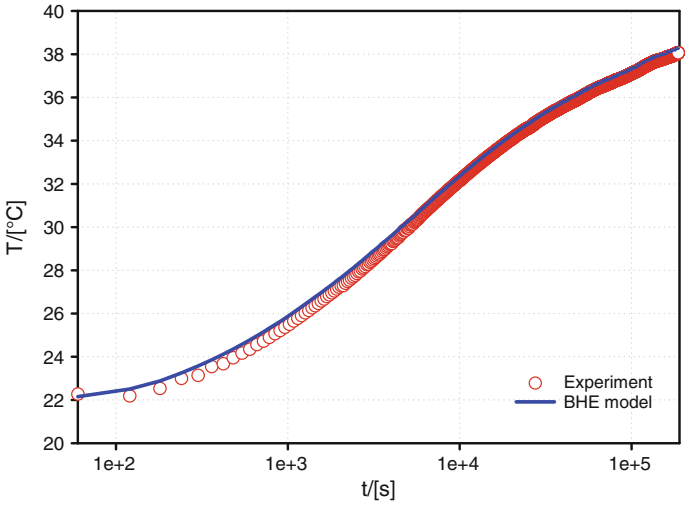

Fig. 2.13 Comparison of simulated and measured outlet temperature profile in the sandbox experiment

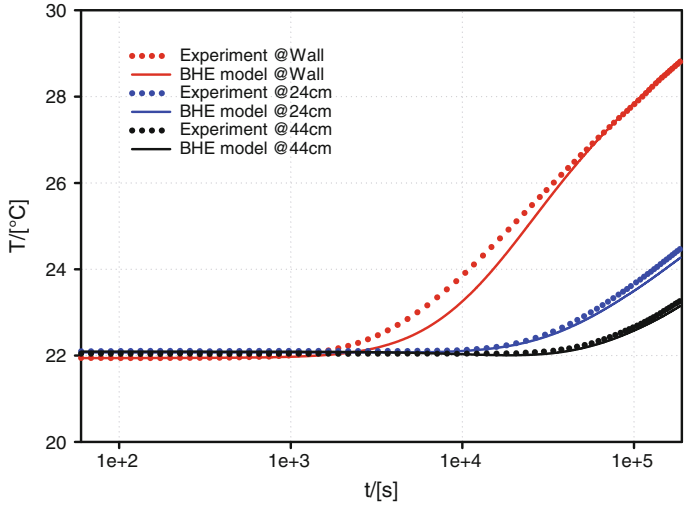

Fig. 2.14 Comparison of modelled and measured wall and soil temperatures

Considering the error of measuring temperatures, flow rate and thermal conductivity values are in the same range, we consider the numerical model to be fully validated.

Requirement on the Mesh

As mentioned in Diersch et al. (2011), when the BHE is represented by 1D elements, the amount of heat flux between the BHE and the surrounding soil is heavily dependent on the size of mesh elements in the vicinity of the BHE node. Diersch et al. proposed a procedure to determine the optimal nodal distance, depending on the number of nodes surrounding the BHE center node as well as the borehole diameter. The optimal distance Δ can be obtained

$$\Delta = ar_b,\ a = e^{\frac{2\pi}{\vartheta}}, \vartheta = n\,tan\frac{\pi}{n} \tag{2.3.2}$$

with r_b the borehole radius and n the number of surrounding nodes. Δ is increasing with n. When designing the mesh, the above equation needs to be considered to ensure the correct heat flux over the borehole wall, since it will control all inlet, outlet and grout temperatures on the BHE nodes. Deviation from Eq. 2.3.2 will lead to inaccurate solutions. In the model at hand, we have $n = 6$ nodes surrounding the BHE center node with a borehole radius of $r_b = 0.065$ m. With Eq. 2.3.2 the nodal distance evaluates to $\Delta = 0.398$ m.

http://www.springer.com/978-3-319-29223-6

Thermo-Hydro-Mechanical-Chemical Processes in Fractured Porous Media: Modelling and Benchmarking
Benchmarking Initiatives

Kolditz, O.; Görke, U.-J.; Shao, H.; Wang, W.; Bauer, S. (Eds.)

2016, XIV, 243 p. 135 illus., 18 illus. in color., Hardcover
ISBN: 978-3-319-29223-6